Supporting Information

Strong，Tough and Conductive Single-Network Hydrogels Based on Deswelling and Salting-out Effect

Xingyue Sun[a], Haiyi Liang[a,c,d*], Lina Ye[b,*]

[a] CAS Key Laboratory of Mechanical Behavior and Design of Materials, Department of Modern Mechanics, University of Science and Technology of China, Hefei, Anhui 230026, China

[b] College of Chemical engineering, Anhui University, Hefei, Anhui 230601, China

[c] School of Civil Engineering, Anhui Jianzhu University, Hefei 230601, China

[d] IAT-Chungu Joint Laboratory for Additive Manufacturing, Anhui Chungu 3D printing Institute of Intelligent Equipment and Industrial Technology, Wuhu, Anhui 241200, China

[*] Corresponding Author

Keywords: osmosis, Hofmeister effects, tough hydrogel

Experimental Section

Materials. Irgacure 2959 (BASF SE), Acrylamide (AAm; 99%; Aladdin), 1-Vinylimidazole (VI; 99%; Aladdin), Acrylic acid (AAc; 99%; Sigma-Aldrich), N-(2-Hydroxyethyl)acrylamide (>98.0%; TCI), κ-carrageenan (Solarbio), Ammonium sulfate ($(NH_4)_2SO_4$; AR; BBI Life Science), Iron(III) nitrate nonahydrate ($Fe(NO_3)_3 \cdot 9H_2O$; AR; Sinopharm Chemical Reagent Co., Ltd), $CuSO_4$ (AR; Sinopharm Chemical Reagent Co., Ltd). All the chemicals were used as received.

Synthesize of hydrogels. The P(AAc-co-AAm) hydrogel was synthesized via UV-triggered radical polymerization. First, photoinitiator Irgacure 2959 (0.1%, w/v of water) and AAm (3.5 M) were dissolved in 15ml deionized water. Then AAc (0.12, 0.15, 0.18, 0.2, molar ratio of AAm) was added into the solution. After adding each reagent, ultrasound was used to disperse them evenly. Afterwards, the homogenous precursor solution was poured into a PMMA mould (75 mm by 55 mm by 3 mm) covered by a quartz sheet, and polymerized by UV light (365 nm, 7.3 mW/cm^2) for 1h to obtain P(AAc-co-AAm) hydrogel (named as P-gel). After removing the reaction template, the as-prepared P-gel was immersed into $Fe(NO_3)_3$ aqueous solution (0.05 M, 0.15 M, 0.2 M, 0.3 M) for 24 h to form F_x-gel, where x represented the molar concentration of Fe^{3+}. Next, the F_x-gel was further immersed into $(NH_4)_2SO_4$ solution (1 M, 1.5 M, 3 M, 4 M) for 2h to form F_x-A_y-gel, where y represented the molar concentration of SO_4^{2-}.

The PHEAA hydrogel and P(VI-co-AAm) hydrogel were synthesized via thermal triggered radical polymerization. For PHEAA hydrogel, all reactants of HEAA (30wt%) and APS (0.1%, w/v of water) were dissolved in deionized water to form precursor solution. For P(VI-co-AAm) hydrogel, VI (1 M), AAm (5 M) and APS (0.1%, w/v of water) were dissolved to form precursor solution. Then the precursor was poured into a PMMA mold covered by a quartz sheet, and kept in oven under 60°C for 8 h to form a gel. Afterwards, the P(VI-co-AAm) hydrogel was soaked in $CuSO_4$ solution (0.1 M) to form P(VI-co-AAm)/Cu^{2+} hydrogel. Finally, both PHEAA and P(VI-co-AAm)/Cu^{2+}

hydrogel were soaked in $(NH_4)_2SO_4$ solution for 24 h.

The κ-carrageenan precursor solution was prepared by dissolving the κ-carrageenan powder in deionized water (0.02 g/ml) under 95°C for 30 min. The solution was poured into a PMMA mould covered by a quartz sheet and cooled to room temperature to form κ-carrageenan hydrogel. Then the κ-carrageenan hydrogel was immersed into $(NH_4)_2SO_4$ solution for 24 h.

Mechanical Test. A universal testing machine equipped with a 50 kg load cell (SUST, China) was used to test all mechanical properties at ambient temperature. Hydrogel samples for tensile measurements were sliced into dumbbell-shape. The tensile speed was fixed at 100 mm min^{-1}. The tensile elongation (λ) was calculated by dividing the distance between clamps by the original length of samples, and the tensile stress (σ, MPa) was measured by dividing the applied force by the cross-section area. The elastic modulus was estimated from the initial slope of σ-λ curve in the range of 1%-3%. The fracture toughness (Γ, kJ m^{-2}) was obtained by separately stretching two samples of the same hydrogel with and without notch to fracture. The original distance between two clamps was fixed at 5 mm. The force-displacement curve was obtained by pulling unnotched samples to fracture. The work, U, was calculated by the area beneath the force-displacement curve. For notched samples, an edge crack of half original width (a_0) was cut by a blade in the middle of the gauge section of the hydrogel sample. A critical distance between two clamps, L_c, was determined when the crack advanced in the notched sample. The fracture energy was calculated by: $\Gamma = \frac{1}{a_0 b_0}\left(\frac{\partial U}{\partial C}\right)_{L_c}$, where b_0 is the thickness of sample. All these measurements were carried out more than three times.

Water Content. Hydrogels for water content measurement were dried to constant weight in the oven. The water content (C_w, wt%) was calculated by $C_w = \frac{w_0 - w_1}{w_0}$, where w_0 and w_1 represent the weight of hydrogels before and after drying. All the tests were repeated more than three times.

Characterization. The rheological measurements of F_x-A_y-gel were conducted by a MCR302 rheometor (Anton Paar). The as-prepared F_x-A_y-gel was cut into a circle with 25 mm in diameter and fixed between measuring head and baseplate using commercial glue. The sample was surrounded by silicone oil to prevent water evaporation. The frequency sweep measurements were conducted under fixed strain of 0.1% and different temperature from 20-90°C. The master curve of storage modulus G' and loss modulus G" were obtained by the time-temperature superposition shifts (TTS) using 30°C as reference temperature. Moreover, the activation energy (E_a) was calculated by the slope of the fitting curve.

Before the freeze drying, the F_x-A_y-gel was immersed in water to wash out the salt solution. Hydrogels prepared for Scanning Electron Microscope (SEM) were first immersed into liquid nitrogen, then transferred into a lyophilizer (Pilot 2-4LD, BIOCOOL) which was cooled to -45°C in advance. After being freeze dried for 3 days, the sample was fractured in the liquid nitrogen to obtain fresh cross section. Before being observed by SEM, the fresh cross section of sample was coated with Au-Pd alloy. Moreover, the freeze-dried hydrogel was used for X-ray Powder diffractometer (XRD) measurements and ground into powder to conduct X-ray photoelectron spectroscopy (XPS) measurements.

Measurements of Electrical Properties. The resistance of hydrogel was recorded by LCR meter (TH2832) at an AC voltage of 1 V. The ionic conductivity was calculated by: Conductivity (S m^{-1}) = $\frac{l}{R*a*b}$, where R, l, a, and b are the resistance, length, width and thickness of hydrogel, respectively. The curve of resistivity with strain ($(R_i-R_0)/R_0$-strain) was obtained by combining the mechanical testing machine and LCR meter during stretching. The gauge factor was calculated by the slope of the $(R_i-R_0)/R_0$-strain curve. Furthermore, the hydrogel was cut into a rectangular shape and connected with metal wires to fabricate a sensor. This sensor was attached to the neck, finger, elbow and knee by cooper tape to detect the movements. The real time resistance change was

recorded by LCR meter. A plastic wrap was used to cover the sensor to prevent water loss.

Supplementary Figures

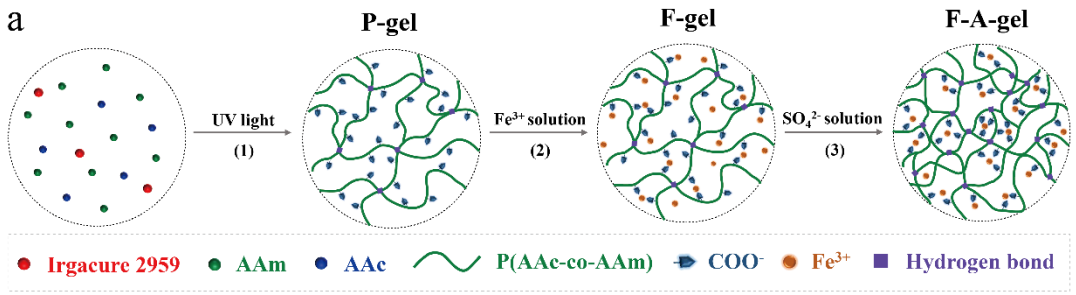

Fig. S1. Synthetic scheme for F-A-gel.

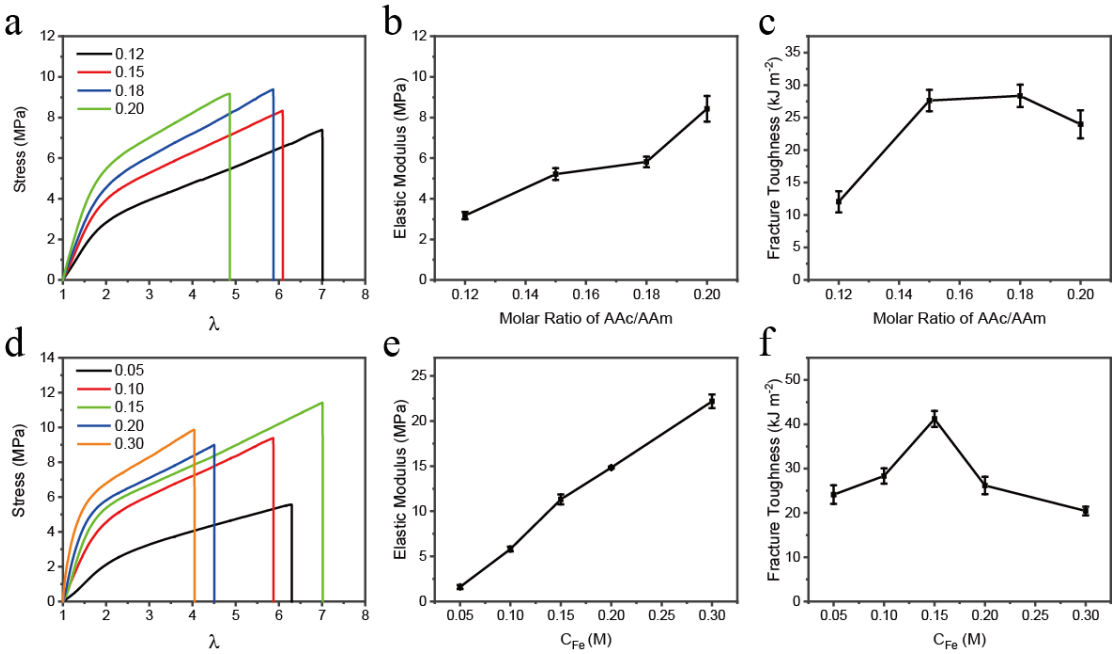

Fig. S2. (a) The tensile behaviors, (b) calculated elastic modulus and (c) fracture toughness of $F_{0.1}$-$A_{2.5}$-gel with various feeding molar ratio of AAm/AAc. (d) The tensile behaviors, (e) calculated elastic modulus and (f) fracture toughness of F-A-gels with different concentration of Fe^{3+}.

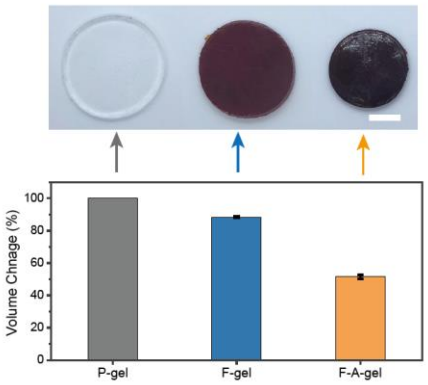

Fig. S3. The photographs and volume change of P-, F-, and F-A-gel. Scale bar: 1 cm

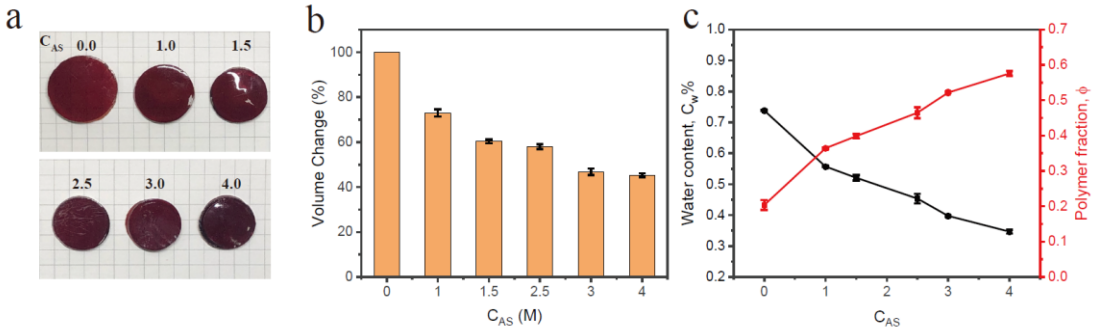

Fig. S4. (a) The macroscopic photos and (b) volume change of $F_{0.15}$-A_y-gel after being soaked in different concentration of $(NH_4)_2SO_4$ solution (C_{AS}). (c) The water content and polymer fraction of $F_{0.15}$-A_y-gel.

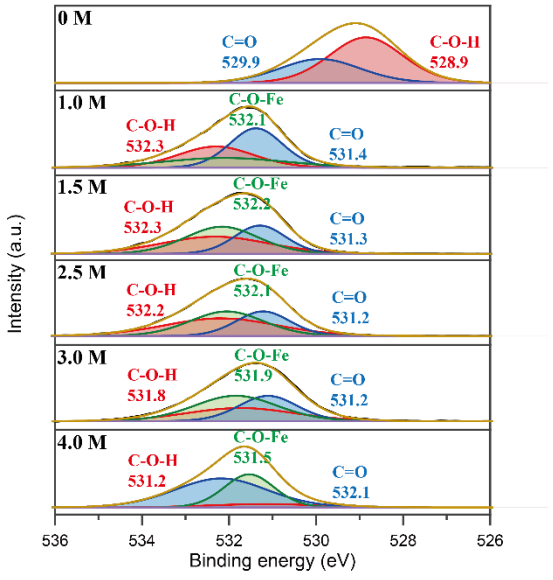

Fig. S5. The XPS measurements of $F_{0.15}$-A_y-gel.

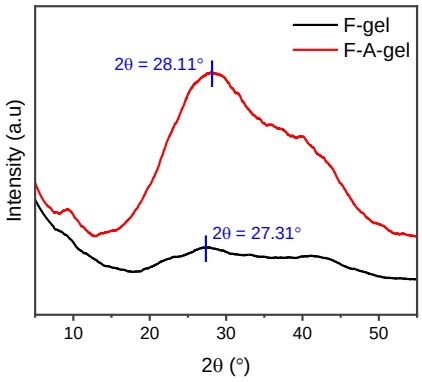

Fig. S6. The XRD patterns of F-gel and F-A-gel.

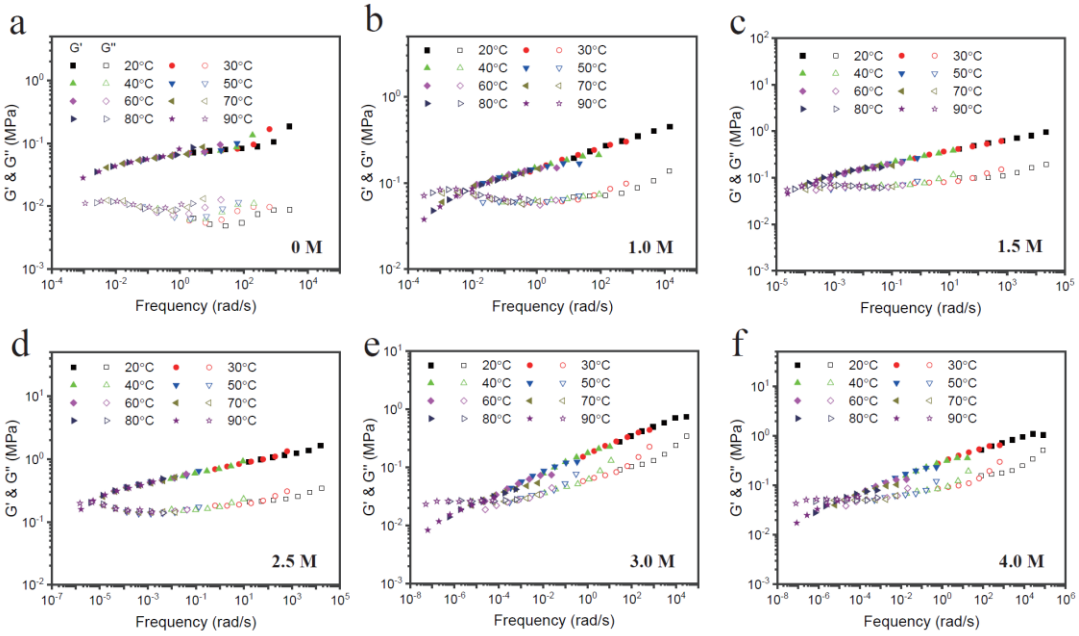

Fig. S7. Frequency sweep measurements of $F_{0.15}$-A_y-gel. The master curves were obtained by time-temperature superposition shifts at a reference temperature of 30°C.

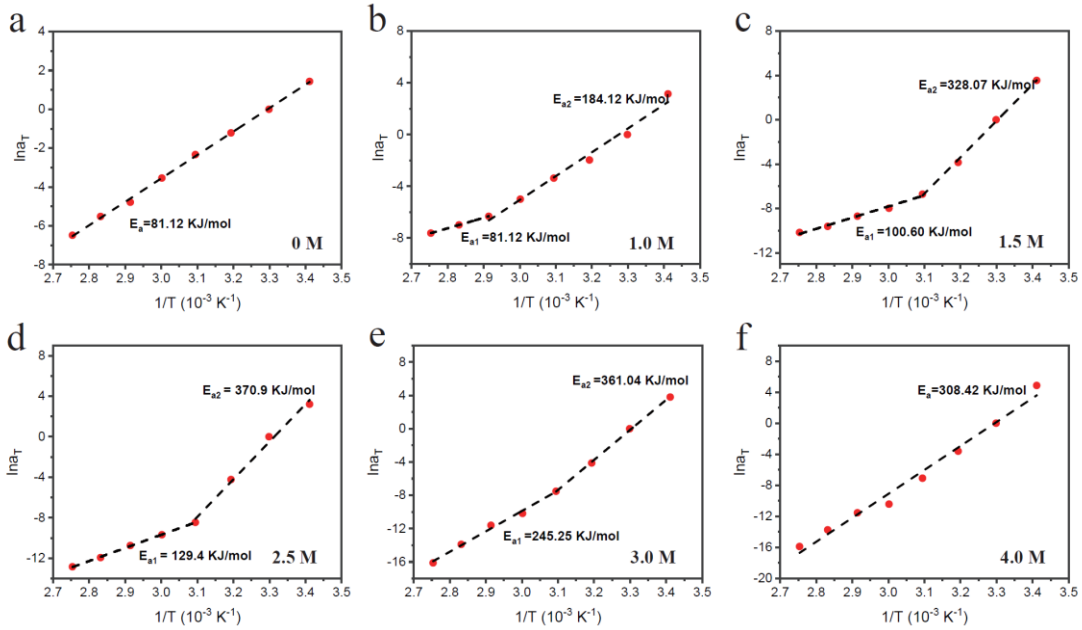

Fig. S8. Arrhenius plot for the temperature-dependent shift factors of different C_{AS}. The apparent activation energy was calculated from the slope of the curve.

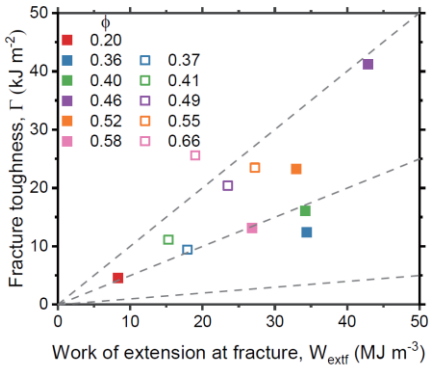

Fig. S9. Fracture toughness (Γ) of F_x-A_y-gel and F_x-D-gel is plotted with work of extension at fracture (W_{extf}). The solid squares are for F_x-A_y-gel while the hollow squares are for F_x-D-gel.

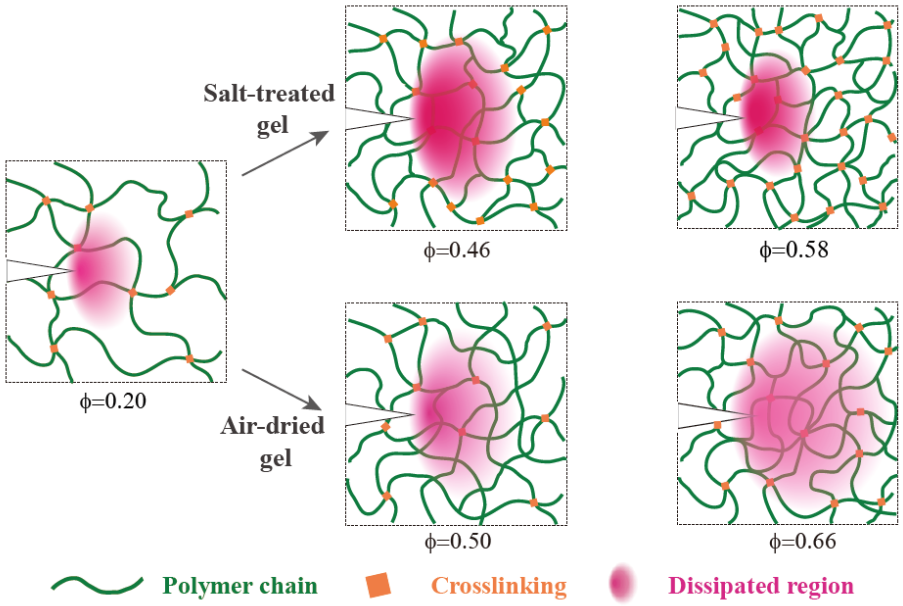

Fig. S10 Structure and toughening mechanism of salt-treated gel and air-dried gel.

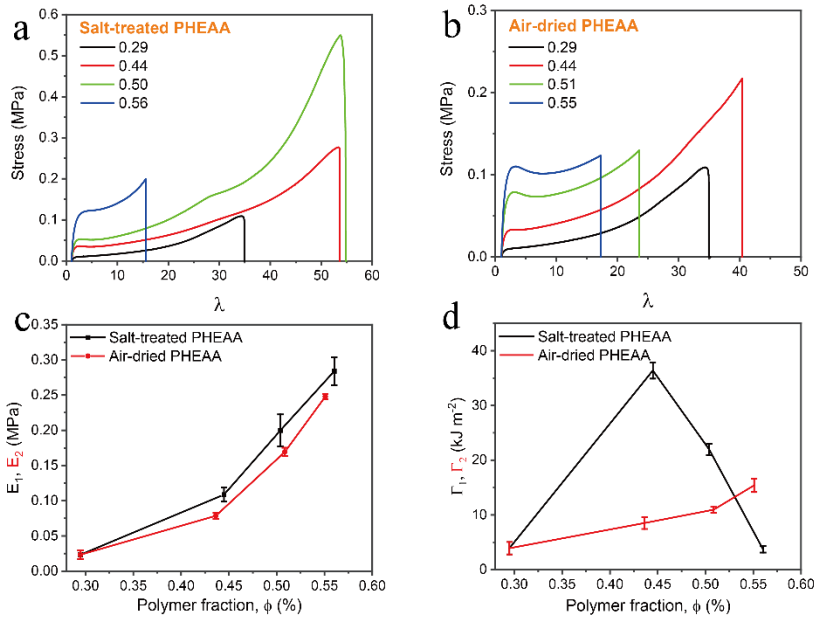

Fig. S11. The tensile behavior of (a) salt-treated PHEAA and (b) air-dried PHEAA hydrogel. (c) The claculated elastic modulus and (d) fracture toughness of salt-treated PHEAA and air-dried PHEAA hydrogel.

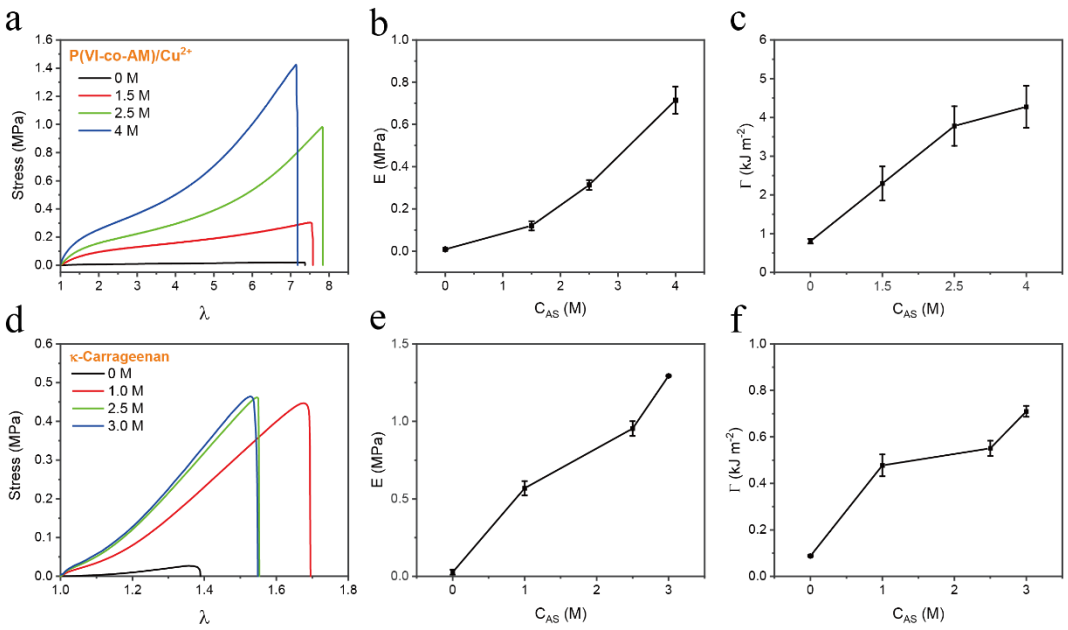

Fig. S12. (a) The tensile behavior, calculated (b) E and (c) Γ of P(VI-co-AAm)/Cu^{2+} hydrogel. (d) The tensile behavior, calculated (e) E and (f) Γ of κ-carrageenan hydrogel

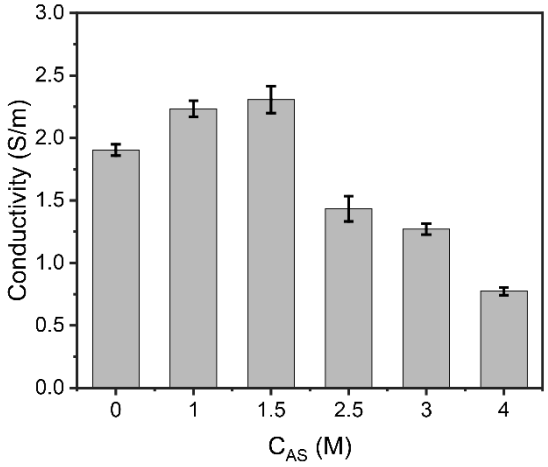

Fig. S13. Ionic conductivity of $F_{0.15}$-A_y-gel.

Molar Ratio of AAm/AAc	C_{Fe} (M)	C_{AS} (M)	Elongation	Tensile Strength (MPa)	Elastic Modulus (MPa)	Fracture Energy (kJ/m^2)	Water Content (wt%)
0.12	0.1	2.5	6.6	6.8	3.2	12.1	55.7
0.15	0.1	2.5	5.9	8.3	5.2	27.6	50.5
0.18	0.1	2.5	6.0	9.2	5.8	28.3	46.7
0.20	0.1	2.5	5.1	8.8	8.4	24.0	43.9
0.18	0	0	8.8	0.02	0.1	1.9	90
0.18	0.05	2.5	6.2	5.3	1.6	24.1	51.2
0.18	0.15	2.5	6.9	11.2	11.3	41.2	45.3
0.18	0.2	2.5	4.7	8.8	14.8	26.2	44.7
0.18	0.3	2.5	4.1	9.7	22.2	20.4	44.5
0.18	0.15	0	6.1	2.8	0.5	4.6	73.8
0.18	0.15	1	6.6	8.8	5.6	12.4	55.7
0.18	0.15	1.5	5.4	8.4	8.6	16.1	52.1
0.18	0.15	3	4.4	12.1	22.1	23.2	39.7
0.18	0.15	4	3.7	13.3	32.9	13.1	34.7

Table S1. The mechanical properties of F_x-A_y-gel.

Sample Code	E (MPa)	λ	σ_b (MPa)	Γ (kJ m^{-2})	C_w (wt%)
F_0-A_0-gel	0.1	8.8	0.02	1.9	90.0
$F_{0.15}$-A_0-gel	0.5	6.1	2.8	4.6	73.8
$F_{0.15}$-A_1-gel	5.6	6.6	8.8	12.4	55.7
$F_{0.15}$-$A_{1.5}$-gel	8.6	5.4	8.4	16.1	52.1
$F_{0.15}$-$A_{2.5}$-gel	11.3	6.9	11.2	41.2	45.3
$F_{0.15}$-A_3-gel	22.1	4.4	12.1	23.2	39.7
$F_{0.15}$-A_4-gel	32.9	3.7	13.3	13.1	34.7
$PHEAA_0$	0.02	34.9	0.1	3.9	69.5
$PHEAA_{2.5}$	0.1	53.4	0.28	36.4	50.0
$PHEAA_3$	0.2	53.9	0.55	22.0	40.4
$PHEAA_4$	0.3	15.6	0.2	3.7	33.6
P(VI-co-AM)/Cu^{2+}_0	0.009	7.4	0.02	0.8	80.9
P(VI-co-AM)/$Cu^{2+}_{1.5}$	0.1	7.5	0.3	2.3	59.0
P(VI-co-AM)/$Cu^{2+}_{2.5}$	0.3	7.8	1.0	3.8	48.9
P(VI-co-AM)/Cu^{2+}_4	0.7	7.1	1.4	4.3	37.8
κ-carrageenan$_0$	0.03	1.3	0.02	0.09	97.8
κ-carrageenan$_1$	0.6	1.7	0.4	0.5	86.2
κ-carrageenan$_{2.5}$	0.9	1.6	0.5	1.6	74.1
κ-carrageenan$_3$	1.3	1.6	0.5	1.7	70.4

Table S2 Summary of tensile properties of the F_x-A_y-gel, $PHEAA_y$ gel, P(VI-co-AM)/Cu^{2+}_y , and κ-carrageenan$_y$ gel.